

# The photoplethysmography-based heart rate variability analysis and calculation of pulse arrival time at different reference points with varying inspiration/expiration ratios

---

**Doctoral (PhD) theses**

**Bella Eszter Ajtay, MD**

**University of Pécs, Medical Faculty, Heart Institute**

**Supervisor: László Hejmel, MD, PhD associate professor**

**Program director István Szokodi, MD, PhD, DSc, full professor**

**Doctoral School director: Lajos Bogár, MD, PhD, DSc, full professor**

**Clinical Medical Sciences Doctoral School**



**Pécs, 2023.**

## Introduction

Photoplethysmography (PPG) is an optically based, non-invasive method that detects blood volume changes in the microcirculation within the cardiac cycle. The technology has been developed for nearly a century. The first landmark was the advent of pulse oximetry in the 1970s. With the appearance of PPG-equipped smart devices in the last 20 years, the number of PPG-related research and publications has rapidly increased. Due to the continuous development in microelectronics, wearables have become an important tool in the field of healthcare, in addition to their everyday convenience. Smart devices equipped with various sensors (PPG sensor, ECG module, accelerometer, gyroscope, barometer, etc.) are capable of recording, storing and sharing large amounts of data from the owner and her/his environment. This offers a huge potential for health monitoring in chronic patients and even for primary prevention in healthy population, as well as high-risk personnel (fireman, military). In order to extract reliable biological information from the PPG signal, it is important to clearly understand, which physiological, environmental and technical factors act on the PPG waveform and how.

The PPG signal consists of an AC component originating from light absorption changes due to the pulsation of arterial blood within cardiac cycles, and a constant DC component originating from the non-pulsating blood and other tissues (e.g. muscle, bone, etc.). The slow changes in the "DC" component are the result of thermoregulation, blood composition and sympathetic nervous system effects, in addition to respiration. In terms of operation, transmissive and reflective type of PPG device can be distinguished. The instrument consists of two main optoelectronic units: a light-emitting diode (LED) and a sensor, usually a photodiode that detects light intensity changes. Besides the ease of use and relatively low cost, its convenience is the main advantage of PPG technology.

Several biological parameters can be derived from the PPG signal. The main application is the pulse detection, where pulse-to-pulse intervals (PPI) are calculated. Wearable devices can indicate a significant difference in the consecutive PPIs, thus they can identify atrial fibrillation. With accurate PPI detection, heart rate variability (HRV) parameters can also be calculated. However, still there is no agreement regarding the equivalence of PPG- and the „gold standard" ECG-based HRV analysis. Some experts suggest that it would be more appropriate to consider pulse rate variability (PRV) as a new

biological indicator. By simultaneous recording of the PPG and ECG signal, we can derive further parameters, including pulse arrival time (PAT) and pulse transit time (PTT) (Figure 1). The PAT is defined as the time required from the electrical activation of the left ventricle to the arrival of the pulse wave at the periphery. PTT is the time, while the pulse wave travels from a proximal point to a distal point in the arterial system. Thus, PAT includes the time of electromechanical coupling of the left ventricle, i.e. the pre-ejection period (PEP). The PAT and PTT values provide important clinical information, inferring arterial wall stiffness. PPG can be used for non-invasive continuous blood pressure measurement (Peñáz pinciple, Finapres).

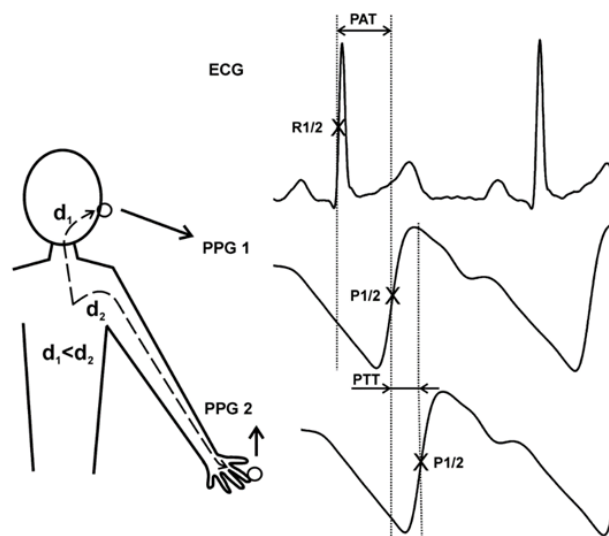


Figure 1. The synchronous ECG and PPG signals acquired at two different locations, the time-delay depends on the distance the pulse wave travels ( $d_1$ ,  $d_2$ ). PPG 1 - earlobe, PPG 2 - fingertip. PAT - pulse arrival time, measured from the ECG reference point to a defined point on the PPG, includes the pre-ejection period and pulse transit time (PTT). PTT - the time of pulse wave traveling from a proximal point to a distal point on the arterial tree. R1/2 - ECG reference point at mid-height of the ascending slope (R wave). P1/2 - the mid-height of the ascending slope (PPG signal).

Heart rate variability (HRV) is the beat-to-beat fluctuation of consecutive R-R intervals (RRI) and is an important non-invasive indicator of cardiovascular regulation and autonomic nervous system function. Physiologically, the current heart rate (HR) is regulated by the sinoatrial node (SN). SN has both sympathetic and parasympathetic innervation (vagus nerve), and their momentary balance influences successive RRIs. The respiratory sinus arrhythmia (RSA) is the beat-to-beat fluctuation of RRIs in synchrony with breathing. HRV is considered an important prognostic factor after myocardial infarction, in arrhythmias or

dilated cardiomyopathy among others. However, a reduced HRV was observed in many other diseases, such as depression and diabetes or other neurodegenerative diseases.

Depending on the length of the recordings, we discern short-term (5 minutes) and long-term (16-24 hours) HRV analysis. HRV parameters can be classified into three main categories: time-domain (TD), frequency-domain (FD) and nonlinear parameters.

The TD parameters are statistical parameters. The simplest TD parameters are the mean RRI (meanNN), the standard deviation of the normal-to-normal intervals (SDNN), the CV% (coefficient of variation,  $SD/mean$ ), and the root mean square of successive interval-differences (RMSSD).

The FD parameters represent the relative (normalized units – n.u.) or absolute ( $ms^2$ ) contribution of each frequency component to the total variability. They can be divided into high frequency (HF: 0.4-0.15 Hz, reflecting parasympathetic actions), low frequency (LF: 0.15-0.04 Hz, both sympathetic and parasympathetic), very low frequency (VLF:  $<0.04$  Hz) bands, and ultra-low frequency (ULF) bands used in the long-term analysis. In addition, the LF/HF ratio reflects the sympatovagal balance.

The Poincaré plot (or Lorentz plot) illustrates the successive RRI ( $RRI_{n+1}$ ) against the actual RRI in a Cartesian coordinate system, resulting in a cloud of points. This area is proportional to the variability of the individual. The cloud can be quantitatively analyzed to calculate the standard deviation of the points along the long (SD-LA or SD2) and short (SD-SA or SD1) axes. Recent quantitative nonlinear parameters are the approximate entropy (ApEn) and sample entropy (SampEn); those describe the complexity and regularity of the RRI time series.

The heart rate asymmetry (HRA) parameters describe the contribution of accelerations and decelerations of the heart rate to its variability, which also reflects the autonomic modulation of the cardiovascular system. In addition to the visual assessment of the Poincaré plot, the level of asymmetry can be quantified by the HRA parameters (Porta index – PI; Guzik index – GI; Figure 2.).

The growing popularity of PPG-based wearable devices in health monitoring requires further improvements in technology and signal-processing algorithms. In PPI detection, choosing the optimal reference point is a crucial step in PRV analysis and PAT calculation.

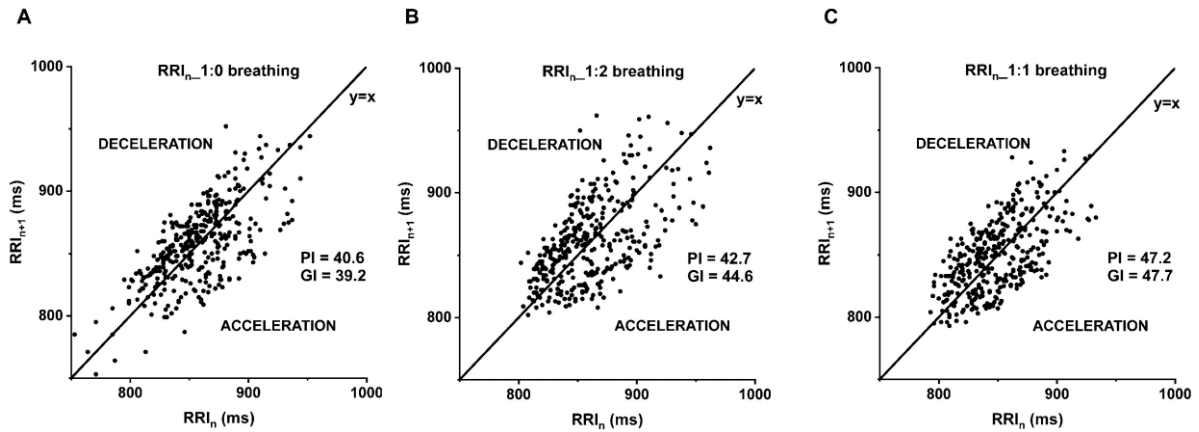


Figure 2. Poincaré plot of *B\_SZ\_29031990* illustrates the more symmetrical distribution of the deceleration and acceleration of the consecutive RR-interval at 1:1 compared to 1:0 and 1:2 inspiration/expiration (i/e) ratio. (A) 1:0, (B) 1:2 and (C) 1:1 ratio breathing. The graph represents the subsequent RR intervals (Y-axis;  $RRI_{n+1}$ ) against the current RR intervals (X-axis;  $RRI_n$ ). Porta-index (PI), Guzik-index (GI), the heart rate accelerates (ACCELERATION) under the identity line, it decelerates (DECELERATION) above the identity line.

As shown in Figure 3, PAT values show a regular beat-to-beat oscillation, which depends on the selected reference point. Standardization of the PPG reference points according to the objectives is essential for comparable studies and accurate measurement.

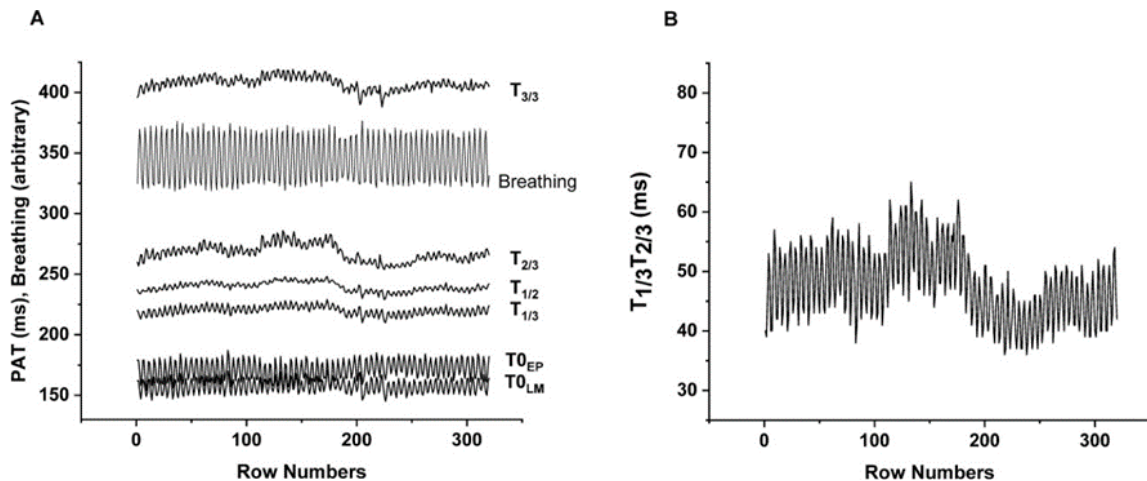


Figure 3. (A) Time series of PATs calculated at different reference points: local minimum ( $T_{0LM}$ ), extrapolated point ( $T_{0EP}$ ), 1/3 height ( $T_{1/3}$ ), 1/2 height ( $T_{1/2}$ ), 2/3 height ( $T_{2/3}$ ) of the ascending slope, local maximum ( $T_{3/3}$ ) and the breathing signal. (B) Time series of the time delay of 1/3 height to 2/3 height ( $T_{1/3}T_{2/3}$ ) points. The breathing-related regular oscillation of the values is evident. Graphs illustrate the PAT values of volunteer MF19970715 at 1:1 breathing ratio.

## **Aims**

This thesis focuses on the following aims:

1. Comparison of the ECG- and PPG-based HRV parameters at different inspiration/expiration (i/e) ratios based on their relative accuracy error (RAE) and the Bland-Altman ratio.
2. Comparing the PAT values at different reference points based on their mean and relative precision.
3. Mathematical description of the relation of corresponding RRIs and PPIs.
4. Actions of different metronome-driven i/e ratios on the HRA and PAT values calculated at different reference points.

## Methods

Our study was approved by the Human Regional Research Ethics Committee (7533-PTE-2018) and involved a total of 50 young, healthy volunteers. In addition, 31 further subjects were enrolled from our other study with the same protocol (7535-PTE-2019). Only physically active individuals aged between 20 and 35 years without taking medication were included in our study. In supine position during the orthostatic adaptation period, the sensors (breathing sensor, self-adhesive ECG electrodes - Einthoven I-II, transmissive PPG sensor on the right earlobe) were installed.

During data collection, simultaneous ECG, PPG and respiratory signals were recorded at different i/e ratios. Four five-minute long recordings were obtained, with the following breathing patterns: 1. spontaneous breathing; 2. metronome-controlled inhalation (1:0); 3. metronome-controlled i/e at 1:2 ratio; 4. metronome-controlled i/e at 1:1 ratio. We defined a breathing cycle of 4500 ms during the guided breathing. Data collection was performed by BioSign HRV-Scanner plus Study version 3.05 (BioSign GmbH, Ottenhofen, Germany). Signals were recorded with a temporal resolution of 1 ms (ECG), 2 ms (PPG) and 20 ms (respiratory signal) in separate files.

We performed the further analysis of the simultaneously recorded 16-bit binary files by HRVScan\_Merge v3.2 software developed by the supervisor (Dr. László Hejmel). After interpolation (cubic spline interpolation to 1ms temporal resolution) and filtering (moving average filter, trend removal filter) the signals, the program merged the four signals phase-correctly into a single file.

The program automatically detected the chosen reference points on the ECG (1/2 amplitude height of the R-wave ascending slope) and PPG signals in each cardiac cycle and calculated the HRV and PRV parameters at each reference point, as well as the beat-to-beat PAT values and their mean and relative precision. The following reference points were defined on the ascending slope of the PPG signal: local maxima ( $T_{3/3}$ ); local minima ( $T_{0LM}$ ); the 1/3–1/2–2/3 amplitude heights ( $T_{1/3}$ ,  $T_{1/2}$ ,  $T_{2/3}$ ) between the previous two points; extrapolated base points by the intersection of the actual linear regression line on the  $T_{1/3}$ ,  $T_{1/2}$  and  $T_{2/3}$  points and the heights of the preceding local minimum; the peaks of the first derivative ( $T_{diff}$ ) as well as the smooth derivative ( $T_{smdiff}$ ) of the PPG signal. The software

automatically calculated the time intervals between the corresponding  $T_{1/3}$  and  $T_{2/3}$  points ( $T_{1/3}T_{2/3}$ ) in every cycle, their mean and relative standard deviation, corresponding to the steepness of the ascending part of the PPG signal (Figure 4).

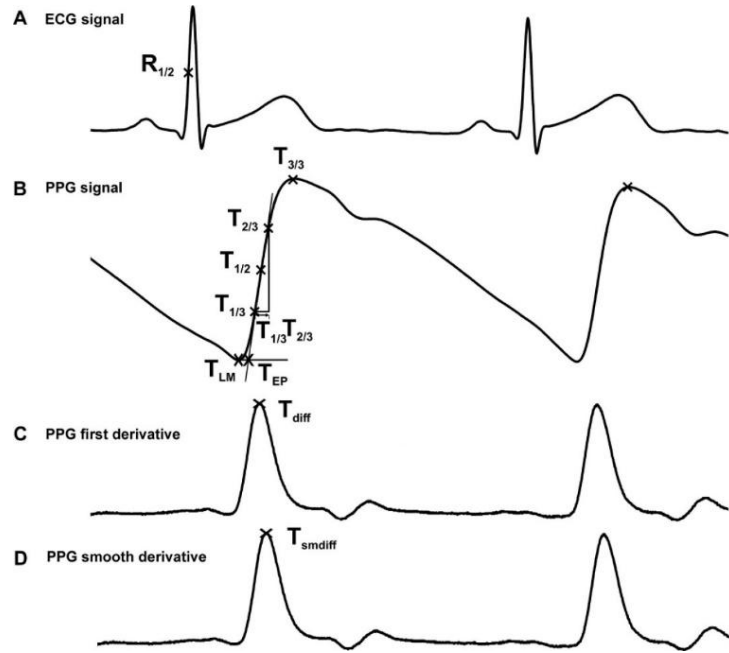


Figure 4. (A) Reference point of the ECG at the 1/2 R-amplitude level on the ascending slope. (B) Reference points of the PPG: local minimum ( $T_{LM}$ ), extrapolated point ( $T_{EP}$ ), 1/3 height ( $T_{1/3}$ ), 1/2 height ( $T_{1/2}$ ), 2/3 height ( $T_{2/3}$ ) of the ascending slope, time interval between  $T_{1/3}$  and  $T_{2/3}$  ( $T_{1/3}T_{2/3}$ ), and the local maximum ( $T_{3/3}$ ). (C, D) The peak of the derivative ( $T_{diff}$ ) and the smooth derivative ( $T_{smdiff}$ ) of the PPG signal (at this magnification, the latter two signals are seemingly identical).

The relative precision (RP%) of the PATs was calculated according to equation eq 1.

$$RP\% = SD/mean \times 100\% \quad (Eq 1.)$$

where  $SD$  is the standard deviation and the  $mean$  is the mean of PAT series from the given reference point.

The HRVScan\_Merge v3.2 software automatically calculated the time domain parameters (meanNN, SDNN, RMSSD, CV%) derived from the ECG and the T1/2 amplitude height of the PPG signal. Kubios HRV Standard 3.5.0. software (Kuopio, Finland) was used to calculate the frequency domain (LF, HF, LF/HF) and nonlinear parameters (ApEn, SampEn).

The accuracy of the PRV parameters was assessed by their relative accuracy error (RAE, %; Eq 2), which was calculated by the following formula:

$$RAE\% = \frac{X_{PRV} - X_{HRV}}{X_{HRV}} \times 100\% \quad (Eq\ 2.)$$

where x is the corresponding PRV or HRV parameter. The RAE% was acceptable below 5%. The ECG- and PPG-based HRV parameters were compared by *Bland-Altman ratio* (BAR) using Origin Pro 2021 software (OriginLab Corp., Northampton, MA). If the BAR is below 10%, the agreement is excellent; the agreement is moderate (10% < BAR < 20%) or insufficient (BAR > 20%).

The HRVScan\_Merge v3.2 program calculated the mean PAT values and ECG-derived HRA parameters (PI, GI) at each metronome-controlled breathing pattern (1:0; 1:2; 1:1) (n=35). We assessed the breathing-related changes in the PAT and HRA values by Friedman's test (p<0.05) and *post hoc* paired Wilcoxon's test, where the modified significance level was set at p<0.01667 based on Holm-Bonferroni correction. The statistical analysis was performed in Microsoft Excel (Microsoft Corporation, Redmond, WA) with StatistiXL package (v.2 .0, 2008, Broadway-Nedlands, Australia).

In a sub-study, we analysed the ECG and PPG records of ten volunteers selected from our database. We calculated the median and interquartile range of respiratory periods at spontaneous breathing, metronome-guided inspiration (1:0), 1:2, and 1:1 i/e ratio, verifying that volunteers followed the breathing protocol correctly. We calculated PATs using the following PPG reference points: T<sub>0EP</sub>, T<sub>1/3</sub>, T<sub>2/3</sub>, T<sub>3/3</sub>, and T<sub>diff</sub>. Fast Fourier transformation (FFT) and normalized cross-correlation analysis was performed on the corresponding RRIs and PAT sequences (Origin Pro 2021, OriginLab Corp., Northampton, MA). We also calculated the frequency shifts of the RRI and PAT spectra. We used Friedman test and *post hoc* paired Wilcoxon test for the statistical comparisons of the results (Microsoft Excel, Microsoft Corporation, Redmond, WA; StatistiXL v.2.0, 2008, Broadway-Nedlands, Australia).

## Results

The final analysis included a total of 35 volunteers' recordings, 21 of whom had an additional spontaneous breathing section as well.

### Comparison of the mean and RP% of PAT values at different reference points

The average PAT values calculated from different reference points are in Table 1. The lowest RP% was found for the PPG ascending slope at  $T_{1/2}$  (2.49%), followed by  $T_{1/3}$  (2.56%) and  $T_{2/3}$  (2.59%). The highest RP% was observed at the PAT calculated from  $T_{0LM}$  (7.14%) and at the local maximum (5.05%). RP% of the different reference points are summarised in Table 2. The  $T_{1/3}T_{2/3}$  interval, which indicates the slope of PPG amplitude, showed a slightly higher RP% than the PATs, averaging 8.38%, due to its lower mean (Table 3).

<b>Breathing pattern</b>	<b><math>T_{0LM}</math> (ms)</b>	<b><math>T_{0EP}</math> (ms)</b>	<b><math>T_{1/3}</math> (ms)</b>	<b><math>T_{1/2}</math> (ms)</b>	<b><math>T_{2/3}</math> (ms)</b>	<b><math>T_{3/3}</math> (ms)</b>	<b><math>T_{diff}</math> (ms)</b>	<b><math>T_{smdiff}</math> (ms)</b>
<b>Spontaneous (n=21)</b>	131.94	154.59	186.84	201.86	219.20	324.84	198.40	195.44
<b>1:0 (n=35)</b>	132.16	158.67	188.91	203.30	219.38	322.36	200.82	198.29
<b>1:2 (n=35)</b>	134.30	161.30	192.98	207.75	224.78	332.47	203.89	201.28
<b>1:1 (n=35)</b>	133.38	161.59	193.98	209.11	226.49	337.26	205.54	202.92

*Table 1. The group-average of the 5-minute-mean PAT values related to different reference points of the PPG signal: local minimum ( $T_{0LM}$ ), extrapolated point ( $T_{0EP}$ ), 1/3 height ( $T_{1/3}$ ), 1/2 height ( $T_{1/2}$ ), 2/3 height ( $T_{2/3}$ ) of the ascending slope, local maximum ( $T_{3/3}$ ), the peak of first derivative ( $T_{diff}$ ) and smooth derivative ( $T_{smdiff}$ ) of the PPG signal, at different breathing patterns: spontaneous breathing (n=21), single-paced (1:0) breathing (n=35), dual-paced for 1:2 (n=35) and 1:1 (n=35) i/e ratio.*

Inspiration/expiration ratio	n	T <sub>0LM</sub> (ms)	T <sub>0EP</sub> (ms)	T <sub>1/3</sub> (ms)	T <sub>1/2</sub> (ms)	T <sub>2/3</sub> (ms)	T <sub>3/3</sub> (ms)	T <sub>diff</sub> (ms)	T <sub>smdiff</sub> (ms)	Átlag (ms)
<b>Spontaneous breathing</b>	21	4.95	3.65	2.50	2.59	2.83	5.33	3.69	3.86	3.68
<b>1:0</b>	35	6.85	3.60	2.63	2.54	2.58	5.07	3.27	3.40	3.74
<b>1:2</b>	35	7.98	3.87	2.56	2.41	2.46	4.70	3.22	3.31	3.81
<b>1:1</b>	35	8.77	3.96	2.56	2.41	2.50	5.07	3.15	3.26	3.96
<b>Average</b>		<b>7.14</b>	<b>3.77</b>	<b>2.56</b>	<b>2.49</b>	<b>2.59</b>	<b>5.05</b>	<b>3.33</b>	<b>3.46</b>	<b>3.80</b>

Table 2. Relative precision (RP%) of the group-average of 5-minute-mean PAT values, calculated at the different reference points at certain breathing patterns. The n is the number of volunteers in the particular group, local minimum (T<sub>0LM</sub>), extrapolated point (T<sub>0EP</sub>), 1/3 height (T<sub>1/3</sub>), 1/2 height (T<sub>1/2</sub>), 2/3 height (T<sub>2/3</sub>) of the ascending slope, local maximum (T<sub>3/3</sub>), peak of derivate (T<sub>diff</sub>) and smooth derivative (T<sub>smdiff</sub>) of the PPG signal, at spontaneous, single-paced (1:0), dual-paced for 1:2 and 1:1 i/e ratio.

Inspiration/expiration ratio	T <sub>1/3</sub> T <sub>2/3</sub> (ms)	RP% (%)
<b>Spontaneous breathing (n=21)</b>	32.36	9.71
<b>1:0 (n=35)</b>	30.47	7.51
<b>1:2 (n=35)</b>	31.80	7.88
<b>1:1 (n=35)</b>	32.51	8.42
<b>Average</b>	<b>31.79</b>	<b>8.38</b>

Table 3. The group-average time interval (T<sub>1/3</sub>T<sub>2/3</sub>) between the 1/3 and the 2/3 height of the ascending slope of the PPG signal at different breathing patterns and its relative precision (RP%): spontaneous, single-paced (1:0), dual-paced breathing for 1:2, and 1:1 i/e ratio.

## Comparison of the HRV and PRV parameters

### *Time-domain parameters*

The mean RAE was below 5% for all TD parameters between ECG- and PPG-derived HRV parameters except RMSSD (5.32%) at 1:2 i/e ratio (Table 4). Based on the Bland-Altman ratio, each of the PPG-TD parameters but RMSSD showed excellent agreement for all i/e ratios, where a moderate agreement (10.48) was found at metronome-controlled 1:2 breathing pattern (Table 5).

Inspiration/expiration ratios	RAE-MeanNN (%)	RAE-SDNN (%)	RAE-CV% (%)	RAE-RMSSD (%)
Spontán légzés (n=21)	<b>&lt;0.001</b>	<b>1.93</b>	<b>1.93</b>	<b>4.28</b>
1:0 (n=35)	<b>&lt;0.001</b>	<b>2.80</b>	<b>2.79</b>	<b>4.23</b>
1:2 (n=35)	<b>&lt;0.001</b>	<b>3.45</b>	<b>3.46</b>	5.32
1:1 (n=35)	<b>&lt;0.001</b>	<b>2.84</b>	<b>2.84</b>	<b>4.41</b>

Table 4. The average relative accuracy error (RAE, %) of the time domain parameters during different breathing patterns: spontaneous, single-paced (1:0), dual-paced breathing at 1:2, and 1:1 i/e ratio. MeanNN – mean RR-interval/PP-interval; SDNN – standard deviation; CV% – coefficient of variation; RMSSD – root mean square of successive RRI/PPI differences The values of RAE < 5% are in bold italics.

Inhalation/exhalation ratio	n	ECG-MeanNN (ms)	PPG-MeanNN (ms)	MeanNN-BAR (%)	ECG-SDNN (ms)	PPG-SDNN (ms)	SDNN-BAR (%)	ECG-CV (%)	PPG-CV (%)	CV-BAR (%)	ECG-RMSSD (ms)	PPG-RMSSD (ms)	RMSSD-BAR (%)
Spontaneous breathing	21	797.75	797.76	<b>0.01</b>	51.48	52.42	<b>2.73</b>	6.44	6.56	<b>2.67</b>	37.32	38.74	<b>5.23</b>
1:0	35	836.21	836.22	<b>0.02</b>	51.63	52.95	<b>7.14</b>	6.24	6.4	<b>6.33</b>	46.4	48	10.48
1:2	35	869.11	869.1	<b>0.02</b>	52.24	53.81	<b>5.56</b>	6.03	6.21	<b>5.2</b>	48.47	50.56	<b>9.03</b>
1:1	35	880.54	880.54	<b>0.01</b>	54.43	55.94	<b>4.96</b>	6.19	6.36	<b>4.9</b>	53.49	55.48	<b>7.53</b>

Table 5. The number of subjects (n), and the average of the time domain parameters from the ECG and the PPG signals and their Bland-Altman Ratio (BAR, %), at different breathing patterns: spontaneous, single-paced (1:0), 1:2 and 1:1 breathing ratio. If BAR < 10%, the agreement is excellent (in bold italics). MeanNN – mean RR-interval/PP-interval; SDNN – standard deviation; CV% – coefficient of variation; RMSSD – root mean square of successive RRI/PPI differences.

*Frequency domain and nonlinear parameters*

The average RAE of the FD and nonlinear parameters was acceptable in the most cases, except for HF ( $\text{ms}^2$ ) and LF/HF ratios (Table 6). As shown in Tables 7 and 8, BAR showed an excellent agreement between ECG- and PPG-derived HF (n.u.) and ApEn regardless of the i/e ratio, and also by LF (n.u.) and SampEn in the most cases. Moderate agreement was observed for LF ( $\text{ms}^2$ ) and HF ( $\text{ms}^2$ ) parameters in most cases. BAR was insufficient ( $20\% \leq$ ) at HF ( $\text{ms}^2$ ) in 1:2, and by LF/HF ratios in 1:2 and 1:1 i/e ratios.

<b>Inhalation/exhalation ratio</b>	<b>RAE-LF(<math>\text{ms}^2</math>) (%)</b>	<b>RAE-LF(n.u.) (%)</b>	<b>RAE-HF(<math>\text{ms}^2</math>) (%)</b>	<b>RAE-HF(n.u.) (%)</b>	<b>RAE-LF/HF (%)</b>	<b>RAE-ApEn (%)</b>	<b>RAE-SampEn (%)</b>
<b>Spontaneous breathing (n=21)</b>	<b>3.16</b>	<b>2.10</b>	5.54	<b>1.72</b>	<b>3.27</b>	<b>2.12</b>	<b>3.32</b>
<b>1:0 (n=35)</b>	<b>4.02</b>	<b>4.97</b>	9.73	<b>2.71</b>	6.71	<b>2.19</b>	<b>3.23</b>
<b>1:2 (n=35)</b>	<b>4.06</b>	5.54	11.59	<b>2.37</b>	7.47	<b>2.33</b>	<b>3.98</b>
<b>1:1 (n=35)</b>	<b>3.97</b>	<b>4.85</b>	9.90	<b>1.99</b>	6.12	<b>2.37</b>	<b>3.73</b>
<b>Average</b>	<b>3.80</b>	<b>4.36</b>	9.19	<b>2.20</b>	5.89	<b>2.25</b>	<b>3.56</b>

*Table. 6. The average relative accuracy error (RAE, %) of the frequency domain and nonlinear parameters during different breathing patterns: spontaneous, single-paced (1:0), 1:2 and 1:1 breathing ratio. The LF (low frequency power) and HF (high frequency power) expressed in  $\text{ms}^2$  and in n.u. were compared by RAE in % units. ApEn – approximate entropy, SampEn – sample entropy. RAE values below 5% are in bold italics.*

Belégzés/ kilégzés arányok	n	ECG-LF (ms <sup>2</sup> )	PPG- LF (ms <sup>2</sup> )	<i>BAR</i> (%)	ECG- LF (n.u.)	PPG- LF (n.u.)	<i>BAR</i> (%)	ECG- HF (ms <sup>2</sup> )	PPG- HF (ms <sup>2</sup> )	<i>BAR</i> (%)	ECG- HF (n.u.)	PPG- HF (n.u.)	<i>BAR</i> (%)
Spontán légzés	21	1124.6	1161.4	<i>10.13</i>	54.74	53.83	<b>4.34</b>	834.4	883.8	<i>13.27</i>	46.93	47.63	<b>3.02</b>
<b>1:0</b>	35	424.7	443.1	<b>9.48</b>	26.94	25.61	<b>9.65</b>	1579.9	1705.0	<i>16.57</i>	73.28	74.97	<b>5.11</b>
<b>1:2</b>	35	449.9	467.4	<i>11.11</i>	27.29	25.94	<b>9.74</b>	1499.5	1644.2	<i>20.51</i>	72.98	74.35	<b>3.48</b>
<b>1:1</b>	35	444.1	462.5	<i>10.81</i>	23.33	22.26	<i>11.16</i>	2023.2	2177.7	<i>16.96</i>	76.63	77.78	<b>3.46</b>
Átlag		610.8	633.6	<i>10.38</i>	33.08	31.91	<b>8.72</b>	1484.3	1602.7	<i>16.83</i>	67.46	68.68	<b>3.77</b>

Table 7. The number of subjects (*n*) and the ECG- and PPG-derived frequency domain parameters and the corresponding Bland-Altman ratio (*BAR*, %, italics) at each different breathing patterns. *LF* (low frequency power) and *HF* (high frequency power) are given in ms<sup>2</sup> and normalized units (n.u.), respectively. If *BAR* < 10 %, the agreement is excellent (bold letter), between 10-20 % moderate, 20 % < insufficient. 1:0 - metronome-controlled inspiration, metronome-controlled inspiration and expiration at 1:2 and 1:1 ratios.

Belégzés/kilégzés arányok	n	ECG- LF/HF arány	PPG- LF/HF arány	<i>BAR</i> (%)	ECG- ApEn	PPG- ApEn	<i>BAR</i> (%)	ECG- SampEn	PPG- SampEn	<i>BAR</i> (%)
Spontán légzés	21	2.63	2.56	<b>9.30</b>	1.08	1.08	<b>5.31</b>	1.57	1.57	<b>8.13</b>
<b>1:0</b>	35	0.38	0.36	<i>15.46</i>	1.04	1.03	<b>5.69</b>	1.49	1.46	<b>7.56</b>
<b>1:2</b>	35	0.45	0.42	<i>22.61</i>	1.07	1.07	<b>5.94</b>	1.59	1.57	<i>10.09</i>
<b>1:1</b>	35	0.36	0.33	<i>24.51</i>	1.01	1.00	<b>6.01</b>	1.47	1.46	<b>9.00</b>
Átlag		0.96	0.92	<i>17.97</i>	1.05	1.05	<b>5.54</b>	1.53	1.52	<b>8.89</b>

Table 8. The number of subjects (*n*). The *LF/HF* ratio and nonlinear parameters, and their Bland-Altman ratio (*BAR*, %). *LF* - low frequency power *HF* - high frequency power; *ApEn* - approximate entropy; *SampEn* - sample entropy. If *BAR* < 10%, the agreement is excellent (bold letter), between 10-20% moderate, 20% < insufficient. 1:0 - metronome-controlled inspiration, dual-controlled i/e at 1:2 and 1:1 ratios.

### The effect of the i/e ratios on the PAT values and HRA parameters

The Friedman test showed a significant difference of PAT values amongst the three triggered breathing patterns. There was no significant difference in  $T_{1/3}T_{2/3}$  intervals. We observed a significant increase in dual-paced compared to single-paced breathing according to the *post hoc* paired Wilcoxon test (Figure 5) at almost each reference points (except:  $T_{0LM}$  at 1:1 versus 1:0).

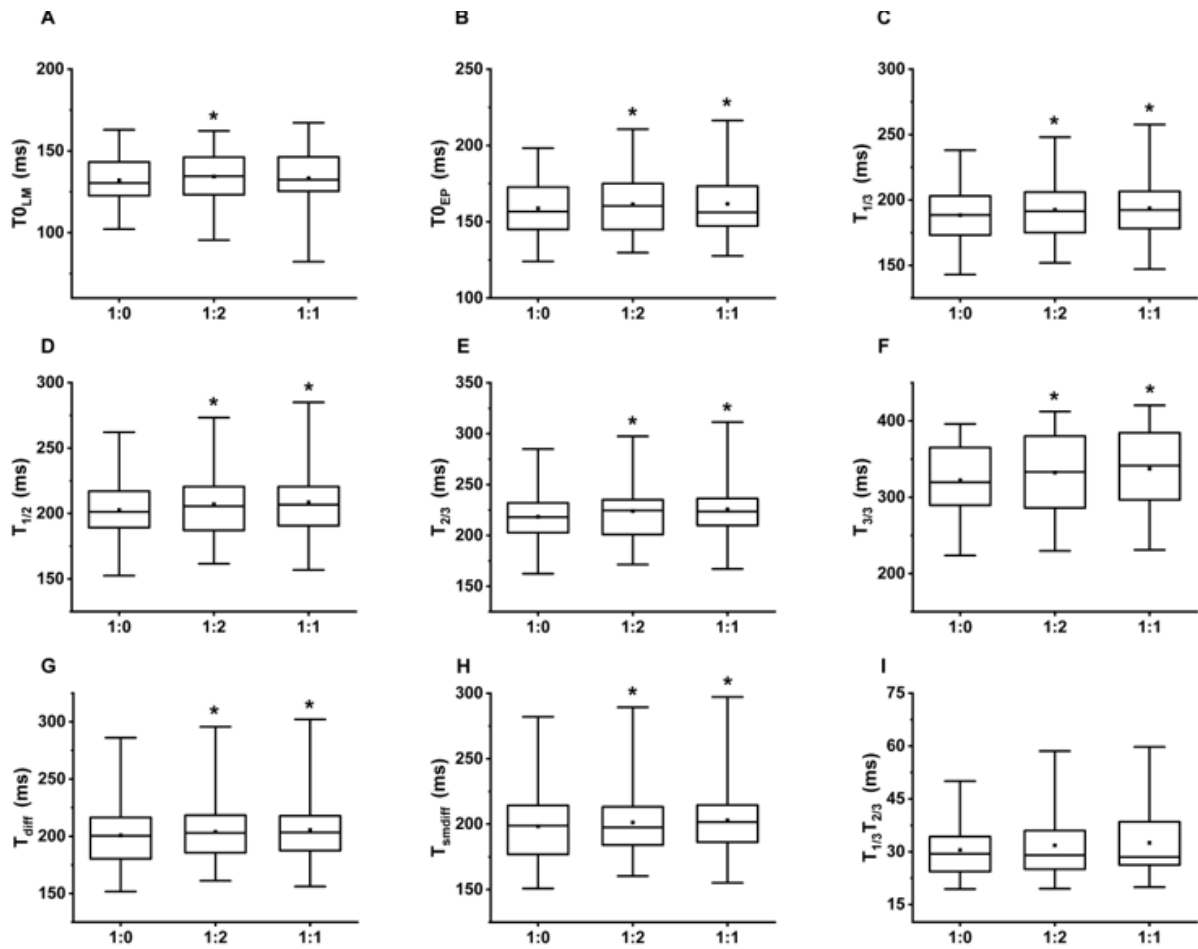


Figure 5. The box and whiskers diagrams represent the mean PAT values at different reference points (A-H). The significant difference compared to single paced (1:0) breathing is marked by \*. The upper and lower sides of the box are the lower and upper quartiles. The box covers the interquartile interval. The horizontal line that splits the box is the median. The small square within the box is the mean. The whiskers indicate the minimum and maximum values in the study population. (A) PAT were calculated at the local minimum ( $T_{0_{LM}}$ ), (B) extrapolated point ( $T_{0_{EP}}$ ), (C) 1/3 height ( $T_{1/3}$ ), (D) 1/2 height ( $T_{1/2}$ ), (E) 2/3 height ( $T_{2/3}$ ) of the ascending slope, (F) local maximum ( $T_{3/3}$ ), (G) the peak of the first derivative ( $T_{diff}$ ) and (H) the smooth derivative ( $T_{smdiff}$ ) of the PPG signal. (I) There was no significant difference in the time interval between  $T_{1/3}$  and  $T_{2/3}$  ( $T_{1/3}T_{2/3}$ ) regarding the i/e.

Regarding the HRA parameters, the *post hoc* paired Wilcoxon test showed a significant increase at 1:1 (symmetric) i/e ratio compared to either 1:0 or 1:2 i/e ratios (Figure 6). In this case, the increase was independent of the number of metronome triggers.

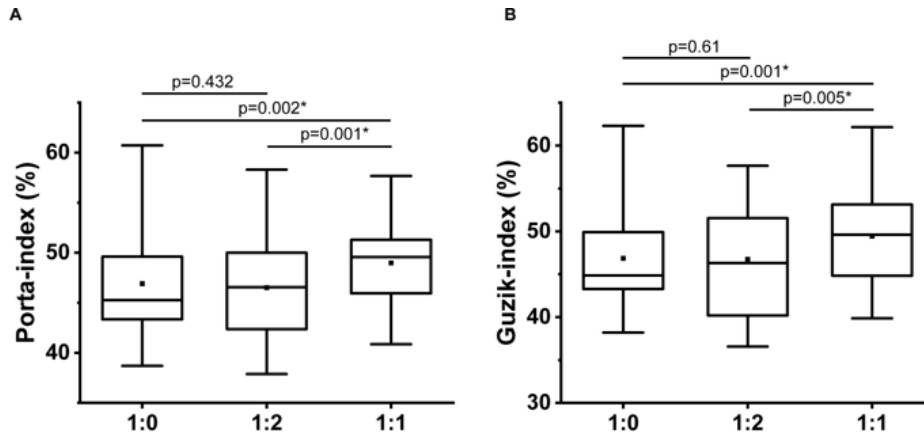


Figure 6. Guzik (A) and Porta (B) indices at single-paced (1:0), 1:2, and 1:1 breathing ratio ( $n = 35$ ); \* indicates the significant difference by post hoc Wilcoxon Paired-Sample test ( $p < 0.01667$ ). The upper and lower sides of the box are the lower and upper quartiles. The box covers the interquartile interval. The horizontal line that splits the box is the median. The small square within the box is the mean. The whiskers indicate the minimum and maximum values within the group.

### The spectral analysis of PAT values

By the normalised cross-correlation of the spectra of PATs and RRIs (from ECG), we found a strong correlation between the PAT and respiratory sinus arrhythmia at each breathing pattern and at most reference points. We found a slightly inferior, but still good correlation between PATs calculated from the local maxima of the PPG signal and their corresponding RRI spectra. The peak identified at 0.22 Hz by spectral analysis of the PAT time series corresponds to the 4500 ms respiration period triggered by the metronome. The frequency shift of the RRI and PAT spectra was 0.00 for each breathing patterns and reference points.

## Discussion

We found an excellent agreement in the most of ECG- and PPG-derived TD parameters according to BAR and RAE% at each breathing pattern. This can be partly explained by the stable reference point ( $T_{1/2}$ ) chosen for pulse detection by PRV analysis, as well as the careful filtering. The trend removal and the moving average filter effectively reduced the reference point jitter due to high-frequency noise and motion artefacts. There was an excellent agreement in the nonlinear parameters. RAE% was below 5 % for most FD parameters as well. The BAR suggests that, in contrast to TD and nonlinear parameters, the calculation of the FD values is not acceptably accurate from PPG records, in spite of appropriate filtering techniques and high sampling frequencies. Based on BAR, LF and HF in n.u. is more reliable compared to them in absolute units ( $\text{ms}^2$ ). Generally, a lower agreement can be observed between HRV and PRV parameters at metronome-paced breathing. The sudden increase after spontaneous breathing at RMSSD can indicate the manifestation of vegetative effects due to triggered breathing.

One of our findings is that the difference between HRV and PRV can be mathematically described by the beat-to-beat oscillation of the  $PAT_n - PAT_{n-1}$  difference. This covers the physiological variability, the effect of the environmental noise corrupting the ECG and PPG signal, and other technical factors. Thus, the difference between the current  $PPI_n$  and the corresponding  $RRI_n$  is the difference between the actual PAT value ( $PAT_n$ ) and the preceding PAT value ( $PAT_{n-1}$ ) (eq 3; Fig. 9).

$$PPI_n = RRI_n + PAT_n - PAT_{n-1} \quad (\text{Eq 3.})$$

The cross-correlation of the spectra of PAT and RRI time series confirmed our hypothesis that there is a strong correlation between PAT and respiratory sinus arrhythmia. The spectral analysis of the PAT values and the  $PAT_n - PAT_{n-1}$  differences shows a peak at 0.22 Hz, which corresponds to the 4500 ms respiration period related to the metronome (Figure 7). This suggests, that the  $PAT_n - PAT_{n-1}$  difference oscillates synchronously with the breathing.

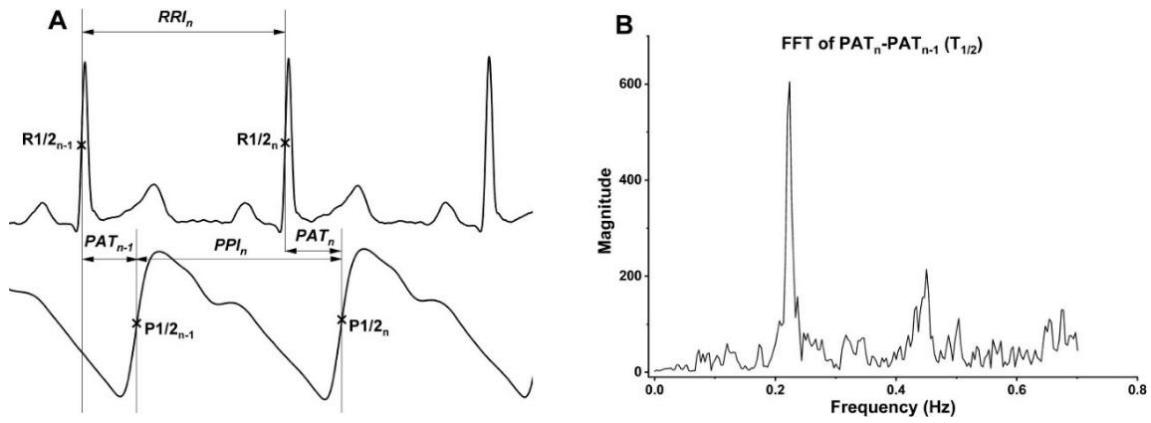


Figure 7. (A) The reference points of the ECG ( $R_{1/2_n}$ ) and the PPG signal ( $P_{1/2_n}$ ) for  $PAT_n$  calculation, in which  $n$  is the serial number of the heart cycle.  $RRI_n$  represents the R-R intervals while the  $PPI_n$  represents the corresponding PP-intervals.  $PPI_n$  can be calculated as  $RRI_n - PAT_{n-1} + PAT_n$ . (B) The Fast Fourier-Transformation of the sequential PAT differences (FFT of  $PAT_n - PAT_{n-1}$ ). Please note the first harmonic at 0.44 Hz in addition to the fundamental breathing frequency due to the asymmetric inspiration-expiration ratio.

A relatively fast action must be responsible for this beat-to-beat fluctuation. The haemodynamic change due to an increase/decrease in intra-thoracic pressure (respiration) affects the left ventricular preload and the actual blood pressure, thus influencing PEP and PTT, and consequently PAT.

The amplitude of the PAT fluctuation varies depending on the reference point. According to our results, the smallest RP% belongs to the PAT values calculated from the  $T_{1/2}$  amplitude height, which is the steepest part of the ascending slope. The signal distortion, the low sampling rate, and the quantisation or external noises result in minimal error in the timing. This can be an important aspect in measurements where motion artifact and/or external noise may be present (e.g. during sport activity).

The PATs calculated from the local maximum ( $T_{3/3}$ ) and from the base point ( $T_{0_{LM}}$  and  $T_{0_{EP}}$ ) showed the most pronounced oscillations, reflecting the physiological effects discussed above. It is important to highlight, however, the higher RP% of  $T_{3/3}$  is partly due to the uncertainty of the peak detection, causing a higher timing error in the peak region. Since the reference point  $T_{1/2}$  shows the smallest fluctuation, it can be considered as the most fixed point of the PPG signal, around which the ascending slope "swings" in synchrony with the respiration (Figure 8). The elongation of  $PAT - T_{0_{LM}}$  is compensated by the steepness of the ascending slope, so there is a reciprocal relation between the PATs calculated from the base point and the  $T_{1/3}T_{2/3}$  interval.

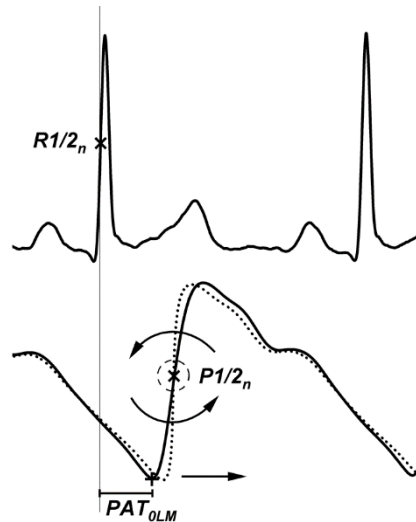


Figure 8. Illustration of the inverse changes in the PAT (calculated from  $T_{OLM}$ ) and the steepness of the ascending slope ( $T_{1/3}T_{2/3}$  interval) in the PPG signal assuring a relatively fixed region at the  $T_{1/2}$  point (“hinge”).

We confirmed a previously published finding by our group that HRA is highly correlated with the length of the inhalation period within the breathing cycle. Consistent with these results, both PI and GI showed a significant increase in symmetric (1:1) breathing compared to 1:0 and dual-paced 1:2 breathing patterns, regardless of the number of auditory signals. Referring to Figure 2, the Poncaré plot shows a more symmetric distribution of beat-to-beat increase and decrease in RRI at 1:1 i/e ratio, due to the symmetric inhalation and exhalation times. In contrast, a significant increase in the mean PAT values occurred related to dual-paced breathing, independently of the i/e ratio. To the best of our knowledge, this phenomenon was first reported by our research group. Even after a thorough review of the literature, we can only limit ourselves to hypotheses, and further studies are needed to clarify the physiological processes behind this phenomenon. During controlled breathing, volunteers were alerted to the start of the inhalation and exhalation by two short auditory signals of different frequencies (1:2 and 1:1 i/e ratio). This process is similar to the oddball paradigm, where the subject has to perform an action according to a discrimination between standard and target cues. By EEG monitoring, the target stimuli are followed by a positive wave with a 300 ms delay. This is known as the P300 potential, which reflects cognitive processes such as attention, short-term memory, stimulus evaluation and related decision-making. Our observation that the PATs are influenced by the number of the metronome-auditory signals suggests a role for higher brain levels and peripheral sympathetic influences in the background.

## Conclusions

The advances and increasing spread of wearable technology have opened new gates in health monitoring. The PPG method has many benefits compared to other heart rate monitoring systems and additionally further biological information can be extracted from the recorded signal. The focus of the present study was to investigate the PPG-based HRV and PAT values and the physiological and technical factors that can influence them. In conclusion, our results show that  $\frac{1}{2}$  amplitude height as the reference point for PPI calculation can provide a reliable alternative to the "gold standard" ECG method for PPG-derived HRV (PRV) analysis in healthy individuals at rest. The difference between the PRV and HRV parameters can be explained by respiration synchronous beat-to-beat fluctuations of the PATs, which covers technical factors in addition to physiological phenomena. The difference in  $PPI_n$  and  $RRI_n$  within a cardiac cycle can be mathematically described with the  $PAT_n - PAT_{n-1}$  difference, which is also associated with respiration. The PAT values calculated from  $\frac{1}{2}$  amplitude height of the PPG show the lowest variability compared to other reference points, due to the steepness of the ascending slope, which is highly resistant to moving artefacts or other noises. This is the most fixed point on the PPG signal around which the PPG slope "swings". The PATs calculated from the base point have the highest RP%, reflecting the respiratory oscillation, while the  $T_{1/2}$  reference point may provide more reliable PPI detection. The aim of the measurement determines the choice of reference point. We observed a significant increase in PATs on dual-paced *versus* single-paced breathing independently of the i/e ratio. We hypothesize that higher brain levels are involved, similarly to the oddball paradigm. Further studies are needed to clarify this hypothesis.

## Novel findings

- We confirmed a good agreement between the HRV and PRV parameters regarding time domain, and the most of the frequency domain and nonlinear parameters in healthy young individuals at rest with spontaneous breathing, and different paced i/e ratios.
- We found that the standard deviation of PAT values is the highest at the TOLM reference point and the lowest at  $T_{1/2}$ , due to the reciprocal fluctuation of the  $T_{1/3}T_{2/3}$  interval with respiration, which is inversely proportional to the PATs calculated at the base point. The oscillation is synchronous with the respiration. The  $T_{1/2}$  point is the most fixed point of the PPG signal, around which the ascending slope "swings". The aim of the measurement determines the reference point selection. The oscillations of PATs can also provide a new non-invasive circulatory parameter.
- Based on our results, the difference between  $RRI_n$  and  $PPI_n$  can be explained by the difference in PAT values between the current and the previous heart cycle, which is also confirmed by a mathematical formula ( $PAT_n - PAT_{n-1}$ ). The PAT series and  $PAT_n - PAT_{n-1}$  show breathing-related oscillations with the same frequency as the respiration, which was verified by spectral analysis. The interchangeability of the HRV and PRV parameters should be investigated in the light of the PAT oscillation.
- The HRA parameters highly depend on the inhalation/exhalation ratio as reported in our previous study, regardless of the number of the auditory signals. On the other hand, we observed a significant increase in the mean PAT during dual-paced breathing compared to single-paced respiration, independently of the i/e ratio. We hypothesise a role of cognitive levels in the background, similar to the oddball paradigm. Our results may provide a good basis for further investigation of stress.

## **Acknowledgements**

I am sincerely thankful to my Supervisor Dr. László Hejjel for his scientific support and essential help, without which my PhD thesis would not have been completed. Furthermore, I would like to thank Prof. Dr. István Szokodi for supporting my scientific career. I also owe my gratitude to Prof. Dr. Attila Cziráki and the staff of the Heart Institute and the Zsigmondy Vilmos Harkány Spa Hospital for their support and enabling my work. Last, but not least, I would like to thank my family and friends who have always encouraged and supported me in my progress.

## Publications of the author

### Original articles the dissertation based on

1. **Ajtay, B. E.**, Béres, S., & Hejjel, L. (2023). The oscillating pulse arrival time as a physiological explanation regarding the difference between ECG- and Photoplethysmogram-derived heart rate variability parameters. *Biomedical Signal Processing and Control*, 79, 104033. <https://doi.org/10.1016/j.bspc.2022.104033> IF: 5.100 (2022), Q1, Cit: 2
2. **Ajtay, B. E.**, Béres, S., & Hejjel, L. (2023). The Effect of Device-Controlled Breathing on the Pulse Arrival Time and the Heart Rate Asymmetry Parameters in Healthy Volunteers. *Applied Sciences (Switzerland)*, 13(9). <https://doi.org/10.3390/app13095642> IF: 2.700 (2022), Q2, Cit: 0

*Comulative impact factors of the original articles related to the dissertation 7.800*

### Oral presentations related to the dissertation

**Bella Eszter Ajtay**, Szabolcs Béres, László Hejjel. Az EKG- és fotopletizmogram (PPG) eredetű HRV paraméterek és a PAT (pulse arrival time). Annual Scientific Congress of the Hungarian Society of Cardiology. Balatonfüred. 13-16 October, 2021.

1. **Bella Eszter Ajtay**, Szabolcs Béres, László Hejjel. A pulzus érkezési idő (PAT) beat-to-beat fluktuációja magyarázza az EKG- és fotopletizmogram-alapú pulzus intervallum eltérését. Annual Scientific Congress of the Hungarian Society of Cardiology. Balatonfüred. 10-13 May, 2023.

### Other publications not related to the dissertation

1. Németh, B., Kiss, I., **Ajtay, B.**, Péter, I., Kreska, Z., Cziráki, A., Horváth, I. G., & Ajtay, Z. (2018). Transcutaneous carbon dioxide treatment is capable of reducing peripheral vascular resistance in hypertensive patients. *In Vivo*, 32(6), 1555–1559. <https://doi.org/10.21873/invivo.11414> *IF: 1.609, Q3*
2. Kreska, Z., Mátrai, P., Németh, B., **Ajtay, B.**, Kiss, I., Hejjel, L., & Ajtay, Z. (2022). Physical Vascular Therapy (BEMER) Affects Heart Rate Asymmetry in Patients With Coronary Heart Disease. *In Vivo*, 36(3), 1408–1415. <https://doi.org/10.21873/INVIVO.12845> *IF: 2.406, Q2*

*Cumulative impact factors: 11.815*